Application of the repulsive-type magnetic bearing technology based on digital control implementation for manufacturing a micro-mass measurement balance system

氏　　名	ALAA ABDEL MONEIM HUSSIEN　MOHAMUD
学位の種類	博士(工学)
学位記番号	博甲第８４１号
学位授与の日付	平成１８年９月２８日
学位授与の要件	課程博士（学位規則第４条第１項）
学位授与の題目	Application of the Repulsive-Type Magnetic Bearing Technology Based on Digital Control Implementation for Manufacturing a Micro-Mass Measurement Balance System （極微小質量計測天秤へのデジタル制御反発形磁気軸受の応用に関する研究）
論文審査委員（主査）	山田　外史（自然計測応用研究センター・教授）
論文審査委員（副主査）	岩原　正吉（自然科学研究科・教授），上杉　喜彦（自然科学研究科・教授）， 神谷好承（自然科学研究科・教授），滑川　徹（自然科学研究科・助教授）

学位論文要旨

Abstract

The repulsive-type magnetic bearing technology is becoming attractive for many applications in recent years, specially, for the high precision instruments. The most important feature of magnetic bearing in general is the contact-free operation. In addition, the repulsive type specially offers many other advantages such as, small number of electromagnets and a simplified scheme are needed for control, it also have a soft and constant stiffness to the passive control axis. So, this type of bearing is right suited for many applications. In this thesis, the repulsive type magnetic bearing based on digital control implementation is employed to manufacture a balance system which can measure micro masses. The proposed system consists of an axial shaft and a balance beam, the shaft is levitated along the radial direction by the repulsive forces of the magnetic bearing section and along the axial direction by a controlled electromagnet. The beam is kept at an equilibrium horizontal position. The principle operation depends on transferring the mass value to the current of a controlled actuator. The function of the system as a mass measuring device is confirmed by measuring some samples and evaluating the system measurement characteristics such as sensitivity, control current hysteresis and linearity.

1. Introduction

It is well known that electronics now provide the 'brains' for today's advanced systems and products, micromechanical devices can provide the sensor and actuator, the eyes and ears, hands and feet which interface to the outside world. For developing both electronics and micromechanical systems, the field of material science has given much of interest. One of the important topics of material science is the material characterization which is performed to specify the physical properties of the materials. The material characterization can be achieved through some chemical analysis such as differential thermal analysis (DTA) and thermograveteric analysis (TGA).

The mass measurement devices which have high measuring sensitivity to detect the minute change of a sample mass are necessary for performing such kind of material characterization analysis. In some applications, the range of that change reaches the order of micrograms or even nano-grams. The important topic to be considered while manufacturing high sensitivity mass measurement devices is the bearing method. The repulsive-type magnetic bearing is a non-contact operation method, so no problem arises from friction which usually affects the system sensitivity. In addition, it is a single-axis controlled system so the number of peripheral devices such as sensors and actuators are

reduced and as a result simple and small size system design is possible. Another important feature of that type of bearing is the soft and constant stiffness to the passive control axis which ensures good levitation stability along the radial direction [1]-[3]. So, for the applications of the earlier requirements, the repulsive-type magnetic bearing is right suited for manufacturing what is called "Repulsive type magnetic bearing micro mass measurement system."

In this thesis, the configuration of the repulsive type magnetic bearing section and forces analysis is given. This section is employed for manufacturing the proposed balance system which consists of two main parts, the axial shaft part and the balance beam part. The complete set up of the proposed balance system and the operating features are included. The system mathematical linearized mode is obtained and controllers for both shaft and beam are implemented around a DSP. The experimental results for confirming the function of the system as a mass measurement device and evaluation of its characteristics such as linearity, accuracy, and precision are given [4], [5].

2. Configuration of the repulsive type magnetic bearing section

2.1 Structure of the PM section

The structure of the repulsive-type magnetic bearing section is shown in Fig. 1 (a). It consists of two units, each unit consists of a cylindrical stator magnet and a cylindrical rotor magnet made from Neodymium-Iron-Boron (Nd-Fe-B) material because of its excellent magnetic properties which are mentioned earlier. The dimensions of both stator and rotor magnets is also illustrated where a piece of magnetic material (90 deg) covers part of the stator magnet in order to improve the repulsive force characteristics as it will be explained later. The stator magnet consists of two pieces attached together. The radial repulsive forces between the stator and rotor magnets make the rotor levitated stably along the radial direction where the axial direction is unstable and needs a controlled electromagnet in order to stabilize the rotor. Due to some manufacturing defects or fabrication difficulties, there is some magnetization asymmetry of magnets and as a result the fabricated magnets of the same material and dimensions are not identical. So, before setting the model, both of the stator and rotor magnets should be selected to be similar i.e. many pieces of rotor and stator magnets should be prepared and the flux density distribution of each piece should be measured in order to select the rotor and stator left and right magnets that have constant flux density distribution around the surface, in addition the flux densities values of both left and right magnets should be as close as possible to each other.

2.2 Finite element analysis of the PM section model

The FEM model of the PM section is shown in Fig. 1 (b) The axial repulsive forces are calculated using the Maxwell 3-D program in order to use this data for designing the electromagnet used for controlling the unstable direction. However, the radial forces are calculated in order to ensure the stabilization along that direction. As shown in the model, both of the left and right stator consists of two pieces of Nd-Fe-B permanent magnet and the stator is covered by a magnetic shunt material.

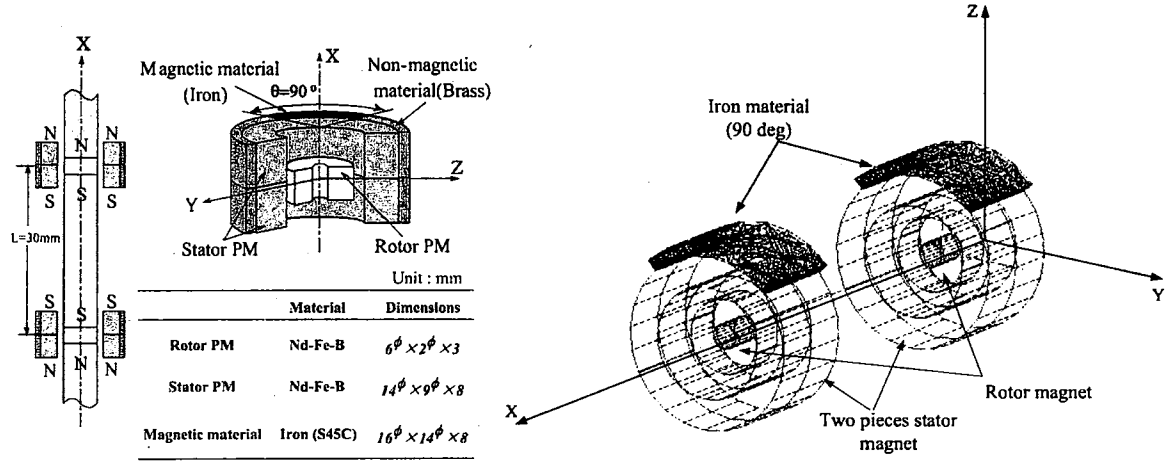

(a) Structure of the section (b) FEM model of the section

Fig. 1 Configuration and FEM model of the PM repulsive type magnetic bearing

The calculated axial repulsive forces in case of using one piece and two pieces stators are shown in Fig. 2 (a) It is clear from the calculated data that the axial force in case of using two pieces stator is less than the force in case of using one piece. In addition the range of force linearity is wider with two pieces. So the stator is designed as two pieces because in this case the force needed for controlling that direction will be less than the force in the case of using one piece, that means small and simple electromagnet design is required. The surface of the upper part of the stator is covered with iron shunt material with different center angles. Two center angles are simulated, 90 degree and 360 degree. Attaching such shunt material affects both axial and radial force characteristics. In Fig. 2 (b), the axial repulsive force without attaching the iron shunt and with iron shunt of center angles 90 degree and 360 degree is shown. The iron shunt of both center angles decreases the axial force, but 90 degree is preferable because of better linearity. Decreasing the axial repulsive force is desirable for a simple control design. Furthermore, this shunt increases the radial repulsive force along z-direction and makes it always positive which is desirable for better stability. This is clearly illustrated in Fig. 3(a) where the radial repulsive force without attaching the shunt and with 90 degree of iron shunt is shown. The negative gradient of the radial force characteristics (i.e. positive stiffness) contribute to passive stability. The radial repulsive force along y-direction is also calculated in both cases(with and without shunt) and shown in Fig. 3(b) The y-direction force changes linearly with the displacement and increases a little when the stator is covered with the magnetic shunt.

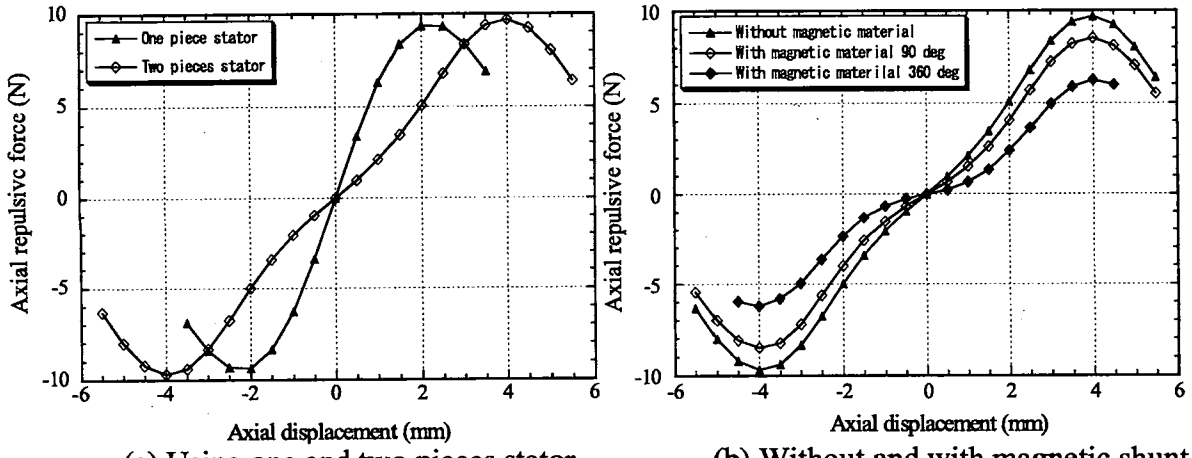

(a) Using one and two pieces stator (b) Without and with magnetic shunt

Fig. 2 Calculated axial repulsive forces characteristics of the PM section.

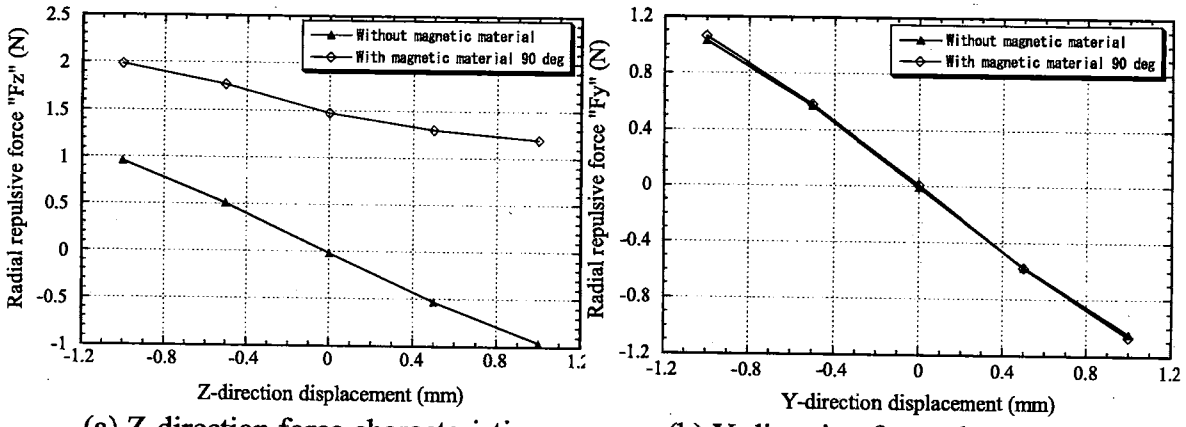

(a) Z-direction force characteristics (b) Y-direction force characteristics

Fig. 3 Calculated radial repulsive forces characteristics of the PM section.

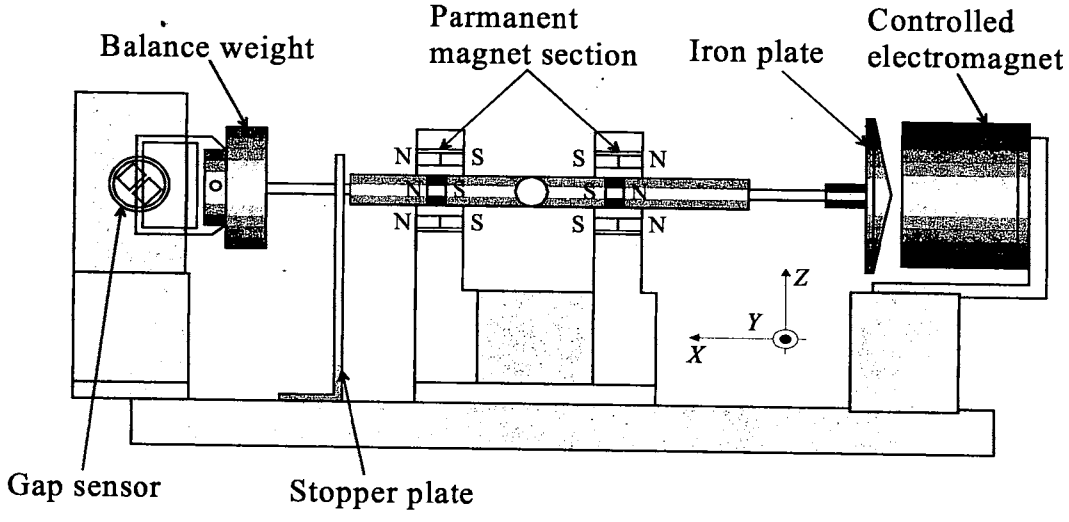

Fig. 4 Configuration of the axial shaft part.

3. Configuration of the axial shaft part

The configuration of the axial shaft is shown in Fig. 4, where the two units of the permanent magnets are installed around the center point; the structure of this section is explained earlier. Based on Earnshaw theorem, the axial shaft is unstable along the axial direction, so a controlled electromagnet is installed to generate an attractive force. This force is modulated through a control system which receives the shaft position information from a gap sensor installed to the left side of the shaft. The explanation of each part individually is given in the next subsections. A stopper plate is placed in order to stop the movement of the shaft while no operation. Furthermore a balance weight is placed at the other end of the shaft in order to keep it in equilibrium position.

3.1 Electromagnet design

The Earnshaw theorem states that, at least, one direction should be actively controlled in order to achieve a stable non-contact levitation in magnetstatic. So, an electromagnet device is installed beside an iron plate fixed in the shaft. The details structure of both Electromagnet and iron plate are shown in Fig. 4 . The EM consists of an iron core and 0.6 mm diameter copper coil of 683 turn, 8.91 ohm resistance and 0.0624 henery inductance. This device is used to generate the required stabilizing force. In fact, the electromagnet causes the flux to circulate in a magnetic loop. When analyzing such magnetic loop, an

exact theoretical computation of the field is rarely possible and seldom required. One usually works with analytic methods of approximation, based on the simplifying assumption that the flux, except for in the air gap, runs entirely through the iron. Since the permeability of iron is considerably larger than that of air, the magnetic field lines leave the iron almost perpendicularly. The EM force can be expressed as follows

$$F = \frac{1}{4}\mu_0 N^2 A_{air}\frac{i^2}{x^2} = K\frac{i^2}{x^2}$$

where N,i are the No. of turns and current of the coil respectively, x is the axial gap, A_{air} is the area of the air gap between the EM and iron plate, μ_0 is the permeability of the air.

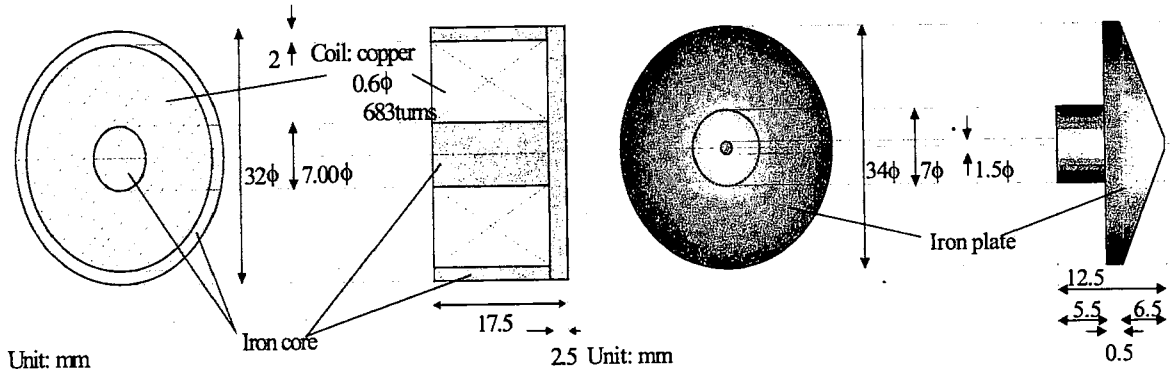

(a) Controlled EM (b) Iron plate

Fig. 4 Configuration of the EM and Iron plate.

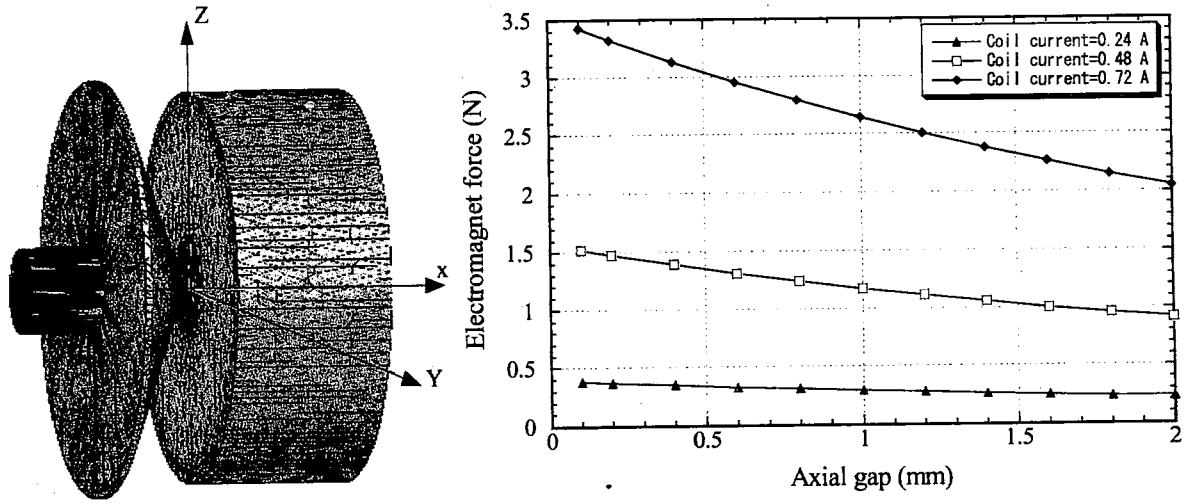

(a) FEM model of the EM (b) EM force characteristics

Fig. 5 The controlled EM model and force characteristics.

The finite element model of the electromagnet device is shown in Fig. 5(a) where the attractive force is calculated as a function of the air gap and the coil current using Maxwell 3-D software. The EM force vs. axial air gap characteristics for different coil currents are shown in Fig 5(b). The axial air gap changes from 0 to 2 mm and the force is calculated at 0.24 A, 0.48 A and 0.72 A current. The force is inversely proportional with the air gap and directly proportional with coil current. In order to achieve a stable non-contact levitation, the EM force characteristics is compared with the PM repulsive force characteristics for determining the steady state operating current and gap. This information is needed for implementation of the control system which is employed to adjust the coil current at the

steady state operating point. The EM steady state operating current is set at 0.48 A and if for any reason, the air gap is changed, the coil current should be also changed in order to keep the EM force constant all the time for achieving stable levitation.

3.2 Axial gap sensor

The optical sensor is fast and has a good sensitivity; in addition, it is magnetically independent, simple and cheap. For these reasons, a photo sensor is used for detecting the displacement of the axial shaft. The structure of the photo sensor is shown in Fig. 6(a), where it consists of a light emitting diode (LED) (GL513F) and a photo diode (PD) (MI-33H2D). The LED emits the light and the shutter obstructs the light. The quantity of the

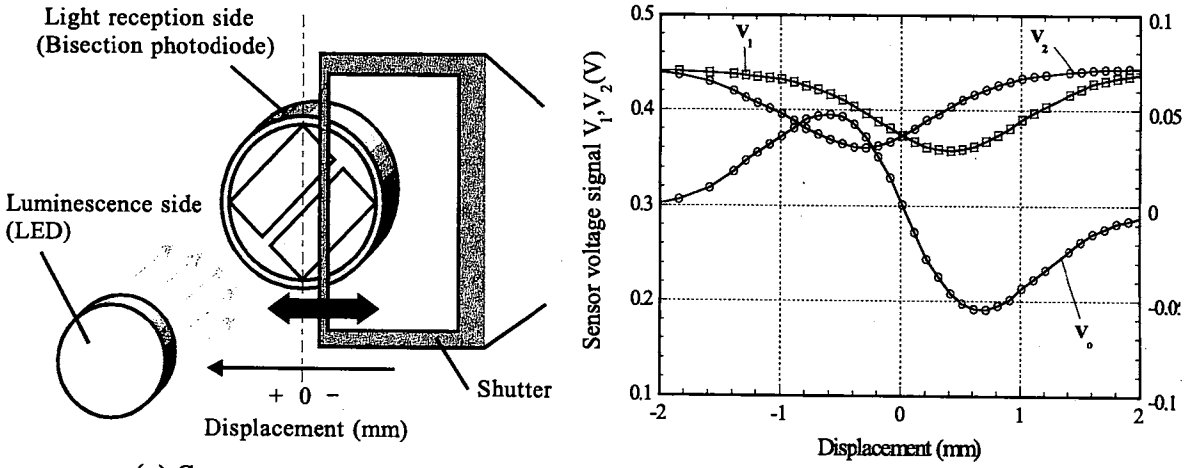

(a) Sensor structure (b) Output characteristics

Fig. 6 the photo gap sensor structure and output characteristics.

incident light on the bisection photo diode is changed as the position of the shaft is changed and as a result the differential output voltage is changed as well. The sensor characteristics is shown in Fig. 6(b)

4. Configuration of the balance beam

4.1 Balance beam with electromagnet actuator

The first trail of manufacturing of the balance beam is shown in Fig. 7 It consists of a brass bar, at on of its ends, an iron ball is attached and at the other end, an aluminum sample holder is placed. A small shutter is fixed at the holder side where a vertical displacement sensor is arranged and installed beside the holder in order to detect the displacement of the beam when the sample is added to the holder. This sensor is the same type of the axial gap sensor used for detecting the axial shaft displacement, but it is only arranged in different way to detect the vertical displacement. The information of the beam position is transferred from the gap sensor to a control system in order to adjust the attraction force of an electromagnet with iron core installed under the iron ball. This EM attraction force is changed as the position of the beam is changed in order to keep the beam in equilibrium horizontal position. As it is explained earlier, the EM reluctance force needed for stabilizing the axial shaft is directly proportional with the square of the EM current and it is same for the EM used for keeping the beam horizontal.

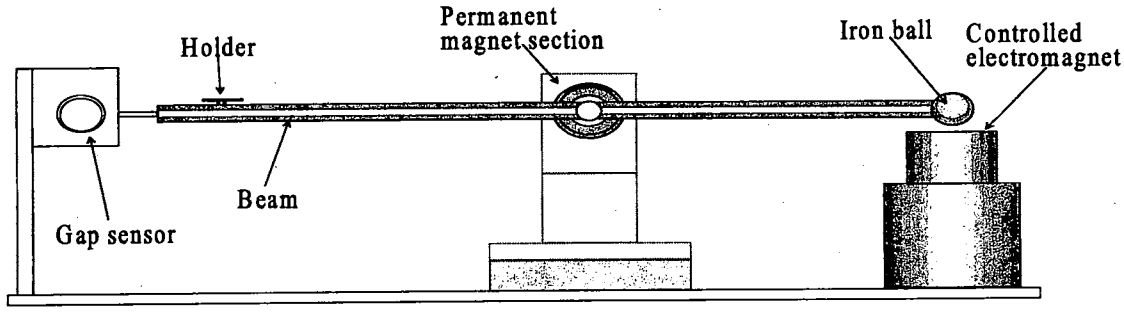

Fig. 7 Balance beam with EM actuator.

A voice coil motor (VCM) actuator is suggested to replace the EM where the stabilizing force is proportional linearly with current. Replacing the EM with this device will increase the system sensitivity which is desired for measuring the small samples. Another important aspect is the saturation of EM iron core and the magnetic hysteresis, it increases the measurement error.

4.2 Balance beam with voice coil motor

The modified balance beam configuration is shown in Fig. 8. The EM and iron ball are replaced by a voice coil motor as the beam actuator to avoid the difficulties in the design and control. Some of these difficulties are the nonlinearity of the EM reluctance force, the complex distribution of the flux in the air gap, and the saturation of the EM core material. The VCM attraction force is linearly proportional with the coil current and as a result, the system measurement sensitivity is becoming higher than in the case of using EM where the force is proportional to the square of the current.

4.3 Structure of the VCM and the flux density distribution

The configuration of the VCM is shown in Fig. 9(a) it consists of an iron yoke, a figure of eight copper coil of 10 turns and 0.6 mm diameter, and two pieces of permanent magnets are attached to the internal sides of the yoke. The permanent magnet is considered as a source of a stationery flux. The force exerted on the coil is given by

$$F_{coil} = B.l.N.i$$

where B is the flux density inside the gap, N is the number of coil turns, l is the length of the part of the coil which lies inside the gap, and i is the coil current. As illustrated in Fig. 9(a), the direction of the force exerted on the coil is upward according to left hand rule. But because the coil is fixed and the yoke is free, there is a reaction downward force exerted on the yoke as given in the equation below. This attraction force exerted on the yoke keeps the balance of the beam.

$$F_m = F_{yoke} = -F_{coil}$$

The simulated magnetic filed distribution of the VCM model by Maxwell 2-D software is shown in Fig. 9(b). The flux density at the line which lies in the middle of the air gap inside the yoke is calculated using the 2-D finite element method. It is clear from Fig. 3-14 that the flux density at that line is parabolic.

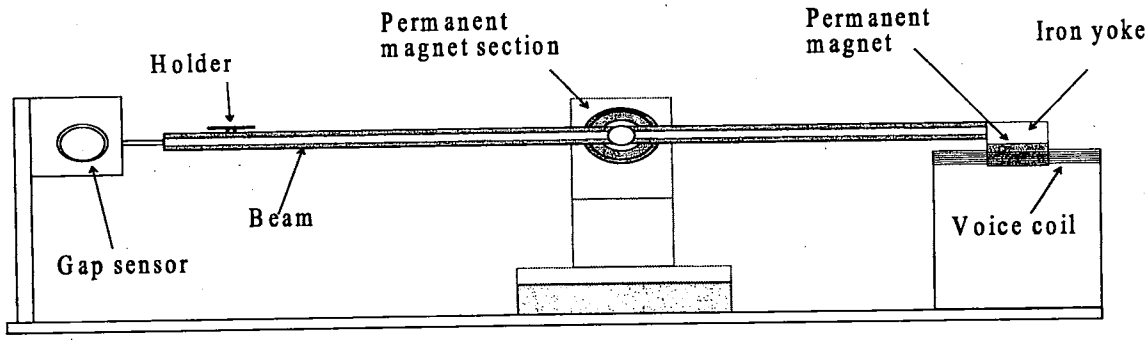

Fig. 8 Balance beam with voice coil motor.

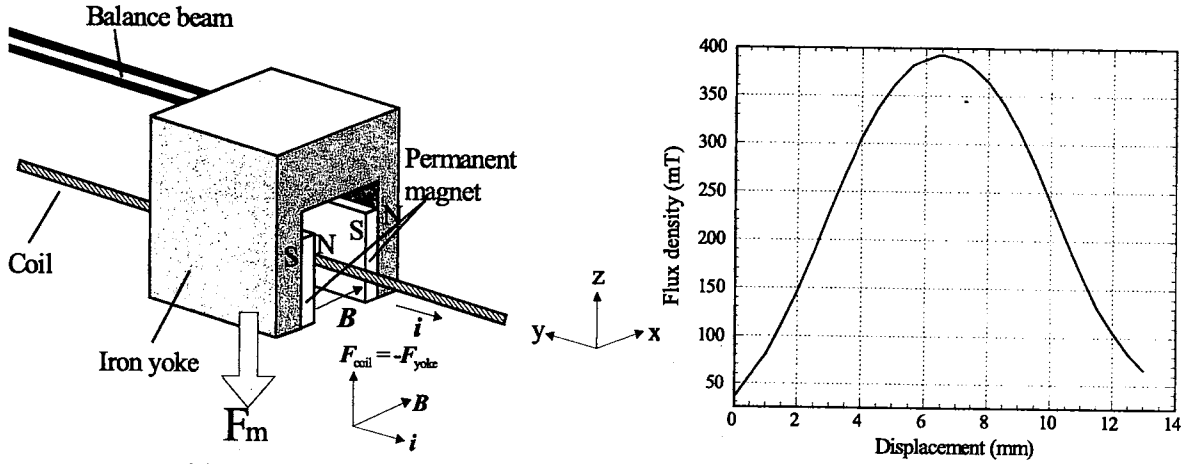

(a) VCM configuration (b) Flux density distribution

Fig. 9 VCM structure and flux density distribution inside the gap at the center

5. Configuration of the complete system and principle operation

The top view of the complete setup of the repulsive type magnetic bearing balance system is shown in Fig. 10. The axial shaft and the balance beam are attached together at the center point. The hybrid magnetic bearing system which includes the permanent magnet units and the electromagnet with active control helps the set to be levitated stably without contact. The most common problem arises in all conventional beam balance is the friction at the fulcrum; this problem decreases the equipment sensitivity. The non-contact levitation of the proposed system overcomes the friction problem seeking for better sensitivity.

The proposed magnetic levitation mass measurement system is based on installing a controlled balance beam and uses it as the measuring device, so the measurement sensitivity is higher than that of the conventional mechanical bearing systems. Also, this system can be used to detect the relative value which is mass where the effect of gravity is eliminated. In some applications, it is needed to detect the mass change of a sample where this change is resulting from heating or pressurization. Since the balance beam of the system is designed so that the sample holder and the actuator are distant enough, it is convenient to be used as a thermo balance which is widely used for the chemical analysis. Some of these analysis such as differential thermal analysis (DTA) and thermo-gravimetric analysis (TGA) are useful for material characterization applications.

The principle operation of the proposed system depends on transferring the additional mass to the actuator control current. When the sample is added to the holder, the beam is disturbed and its position is changed. The vertical displacement of the beam is detected by the gap sensor installed beside the holder and by the help of digitally implemented control system; the actuator control current is changed in order to generate the force needed to keep the beam at its original position.

The function of mass measuring is confirmed by adding some samples to the holder and noticing the voice coil current change. In order to prove that the system measures the correct sample mass, some samples of known masses are also measured after calibrating the system. The details of experimental results of measurement and the evaluation of the system measurement performances such as linearity, accuracy, precision and repeatability will be given later.

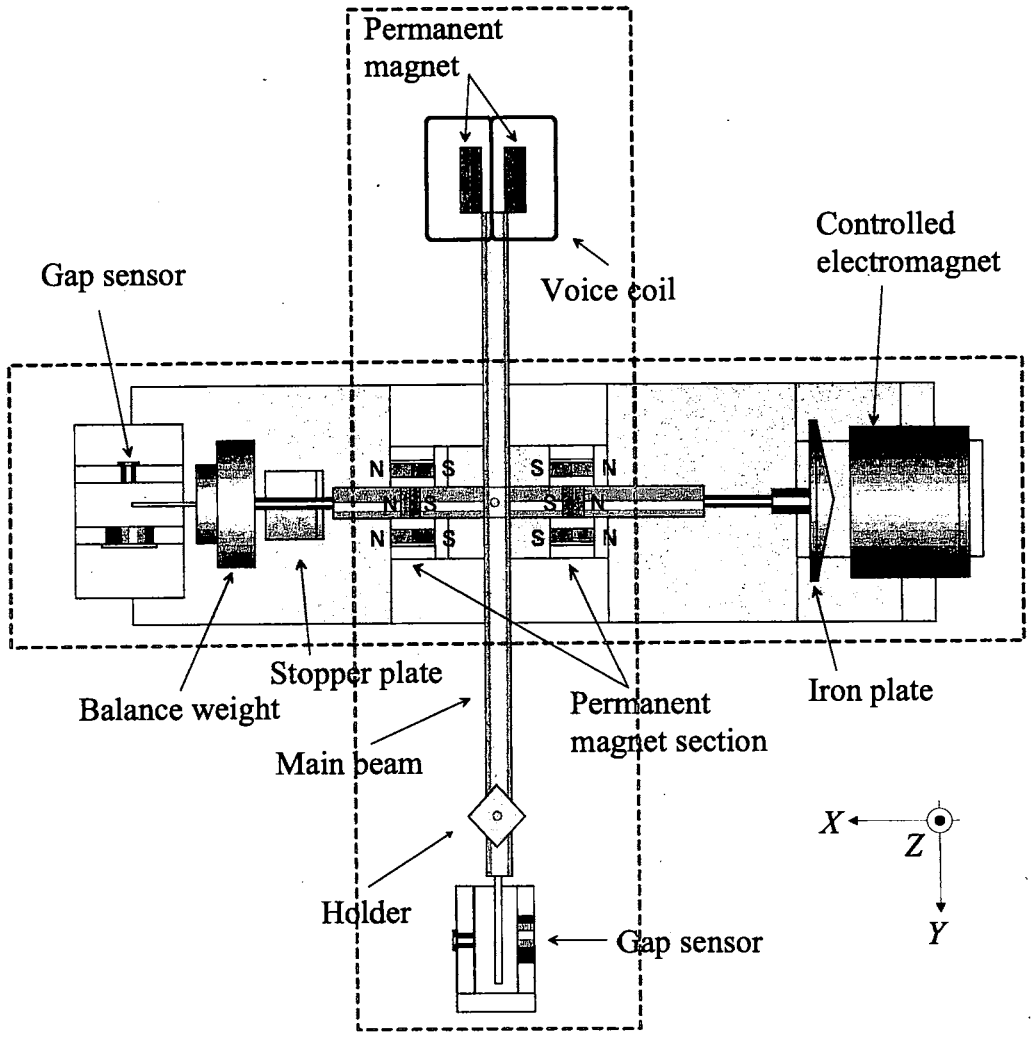

Fig. 10 Top view of the complete setup of the proposed balance system.

6. System modeling and control design

6.1 Analytical models of the axial shaft and balance beam

The dynamic model of the axial shaft is shown in Fig. 11(a). For deriving a simple system model, some ideal conditions are assumed. These conditions include no leakage flux, no DC magnetic saturation or hysteresis in the electromagnet, however, the permeability of the core is assumed to be infinity. The differential equations which describe the motion of the levitating object are derived as follows:

$$m\ddot{x} = F(x) - F_m(x,i) \quad , \quad Ri + L\dot{i} = e$$

where $F = K\left(\frac{i^2}{x^2}\right)$ and $F = ax + b$

The analytical model of the balance beam should be also derived in order to design the beam controller. The physical laws which govern the motion of the beam are investigated where the model is shown in Fig. 11(b)

$$m_1\ddot{z} = m_2 g - m_1 g - F_m(z,i) \quad , \quad m_1\ddot{y} = 0 \quad , \quad Ri + L\dot{i} = e$$

where $F_m = N \cdot i\, B l_2$

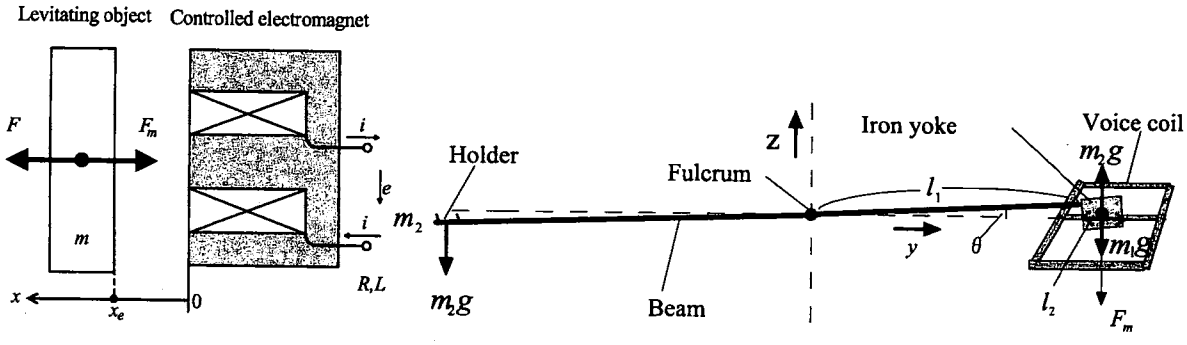

(a) Shaft model (b) Beam model

Fig. 11 Analytical models of shaft and beam

6.2 Ccontroller implementation

After the analytical models of both shaft and beam are derived and the state space equations are obtained, the controllers are designed using the linear quadratic optimal control technique where the block diagram of shaft and beam control systems are shown in Fig. 12. The block diagram of the whole system with control is given in Fig. 13 where 4-channel, 12 bit, 25 KHz analog-to-digital converter receives the voltage signals from both of the axial and radial gap sensors which express the displacement of both shaft and beam. These voltage signals are fed to the controller after it is being converted into displacement signals. The controller output is passed to the digital-to-analog converter and then the control signals are fed to the magnetic bearing actuators (EM and VCM) through power amplifier circuits.

The control process starts with running the MTALAB program to calculate the controller feedback matrices and then generating the real-time control signals by executing the MTALB SIMULINK controller model. By the help of μ-pass software, the executed data is submitted to the DSP and after that the magnetic bearing system is operated. It is confirmed that the previously designed controllers could achieve stable levitation of the system along the axial direction where the beam could be kept at an equilibrium horizontal position even after it is subjected to external disturbance.

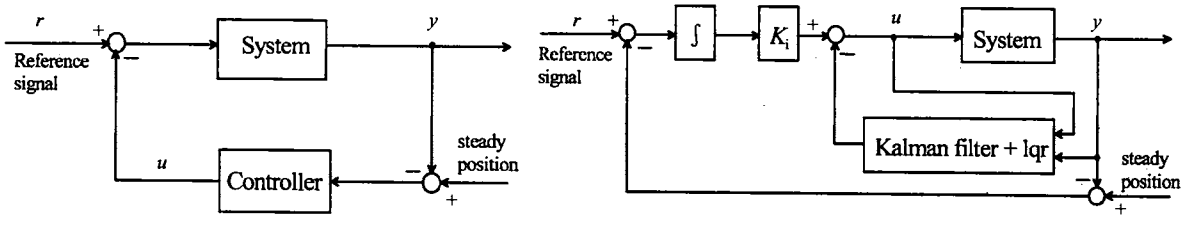

(a) Shaft control system block diagram (b) Beam control system block diagram

Fig. 12 Block diagram of the control systems

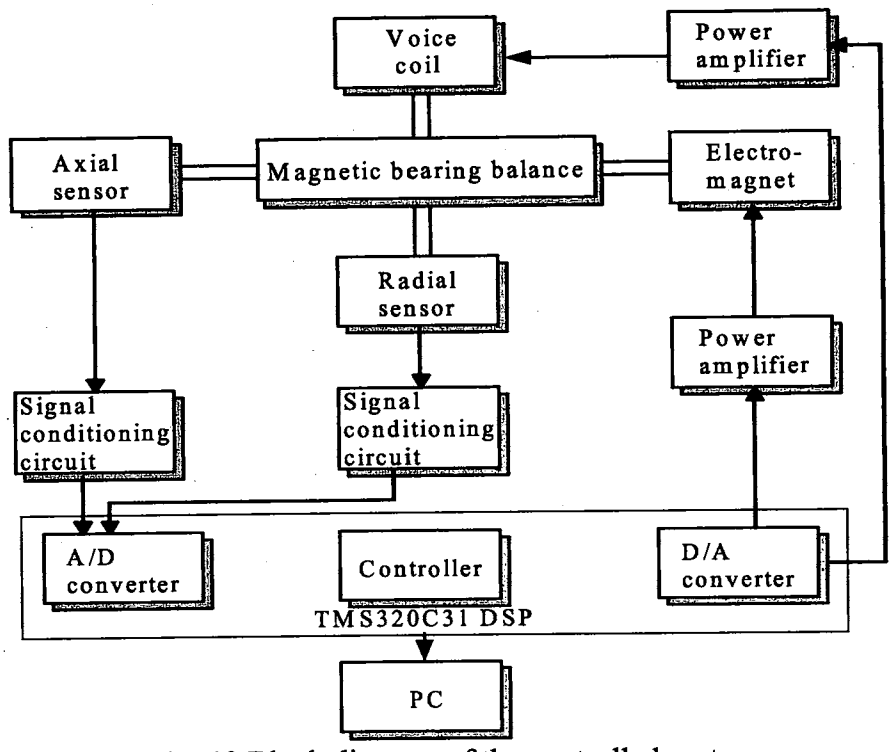

Fig. 13 Block diagram of the controlled system

7. Mass measurement and evaluation of the system performances

After the system is manufactured and the controllers are designed and implemented around a DSP, the experiments are carried out on the system to confirm the function of mass measuring and evaluate the performances. In the first experiment, some samples of equal masses are added gradually to the mass holder and removed by the same way. In each time the control current is noticed. The control current vs. sample mass characteristics is shown in Fig. 14(a) where the beam actuator is an EM with iron core. The control current variation is increased as the sample mass inside the holder is increased. As shown in Fig 14 (b), the difference in the control current between the increasing direction and decreasing which is defined by the hysteresis is investigated by zooming into Fig 14 (a). It is found that the sensitivity is quite low and the value of the hysteresis is equivalent to 730μg. and the non-linearity error of the characteristics is about 5% of the full scale current.

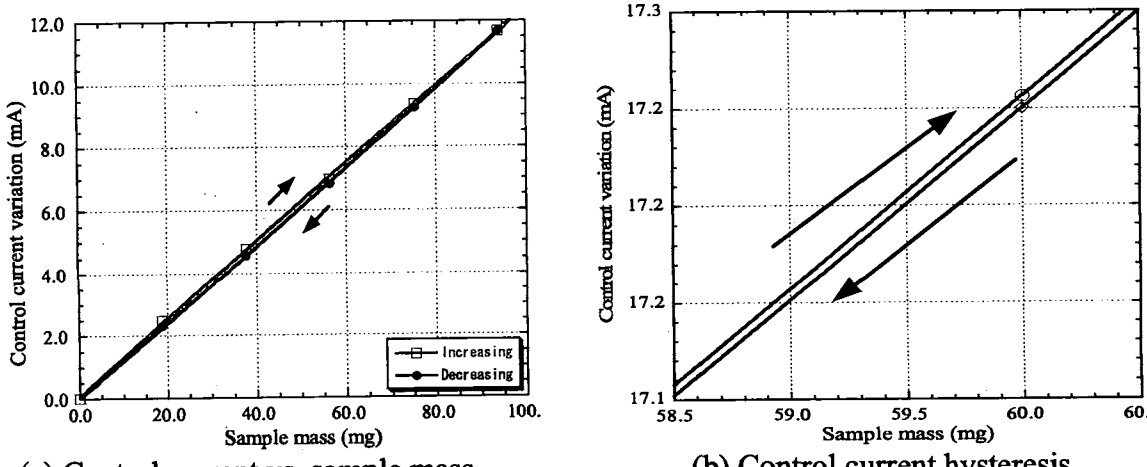

(a) Control current vs. sample mass (b) Control current hysteresis

Fig. 14 Control current vs. sample mass characteristics (beam actuator is EM)

8. Improvement of the system measurement characteristics

8.1 Replacing the EM beam actuator by a voice coil motor

Because the EM force is proportional to the square of the coil current and the problems arise from iron core saturation, the system measurement characteristics are not satisfactory. The EM is replaced by voice coil motor device where the force is proportional to the coil current and the source of the flux is permanent magnets (PM's). In order to keep uniform flux density inside the yoke gap for certain range along the center, some permalloy films are attached to the surface of the PM's; this help for decreasing the current hsteresis. By the same way the experiments are carried out on the system and samples of equal masses are added gradually and removed. The control current vs. sample mass characteristics is shown in Fig. 15(a). It is found that the system sensitivity is increased to more than two times; the hystersis is decreased to 10μg and the nonlinearity error to about 1%. Also the readability of the system was about 75μg as illustrated in Fig. 15 (b).

8.2 Replacing the equal arm brass beam by unequal arm Duralumin beam

In order to increase the system readability and sensitivity which is the main objective for proposed system the equal brass beam brass beam is replaced by unequal arm beam made from Duralumin which is light and stiff material. The arm length to the holder side is becoming double the arm length at the actuator side, and the flat mass holder is replaced by a knife-edge one. After this modification, the system sensitivity is doubled as shown in fig and the nonlinearity error is decreased to 0.2% as shown in Fig. 16(a) where the readability reached 30μg as shown in Fig 16(b). Another experiment is carried out on the system to evaluate its accuracy and precision where the reading of the system is compared by the reading of a Mattler Toledo balance AB204-S (220g×0.1mg). In this experiment some sample of different masses in the range from 0-100mg are prepared and measure, first by Mettler Toledo balance and then by the proposed system. As shown in Fig. 17 (a), the maximum difference in the reading between the two systems was 0.2mg. In another experiment each sample is measured by the proposed system many times and the standard deviation is calculated. It is found that the maximum deviation was about 0.1mg as given in Fig 17(b).

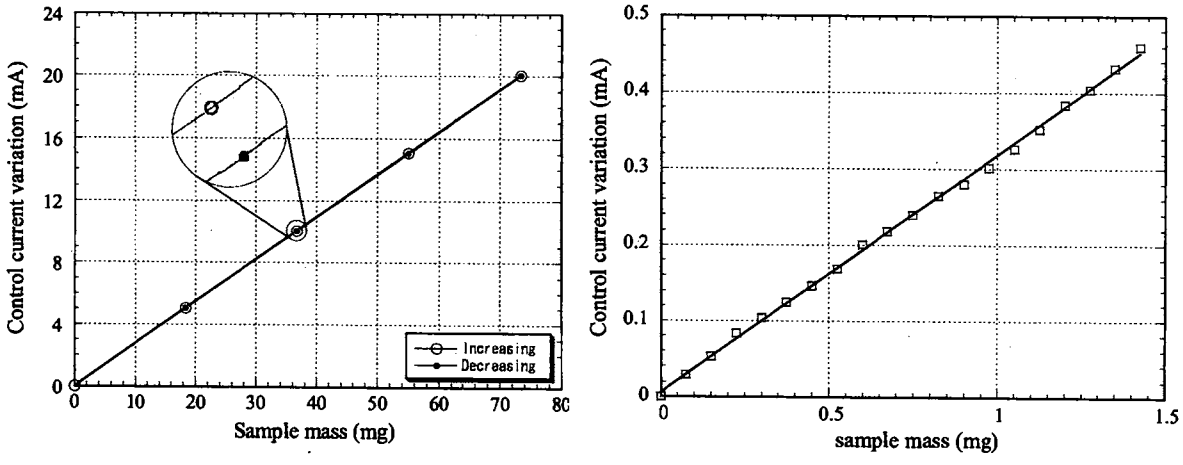

(a) Characteristics for the normal range (b) Characteristics with step of 75μg

Fig. 15 Control current vs. sample mass characteristics (beam actuator is VCM).

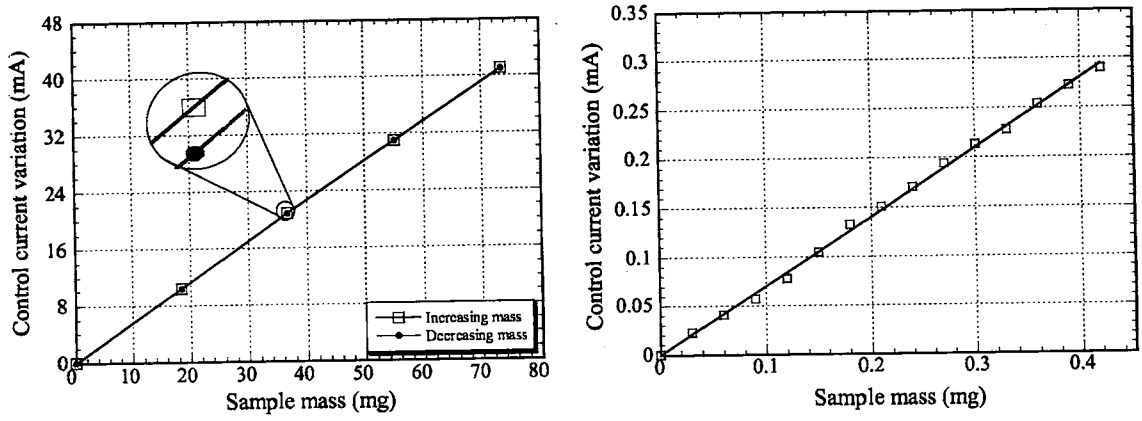

a) Characteristics for the normal range (b) Characteristics with step of 30μg

Fig. 16 Control current vs. sample mass characteristics using unequal arm Duralumin beam

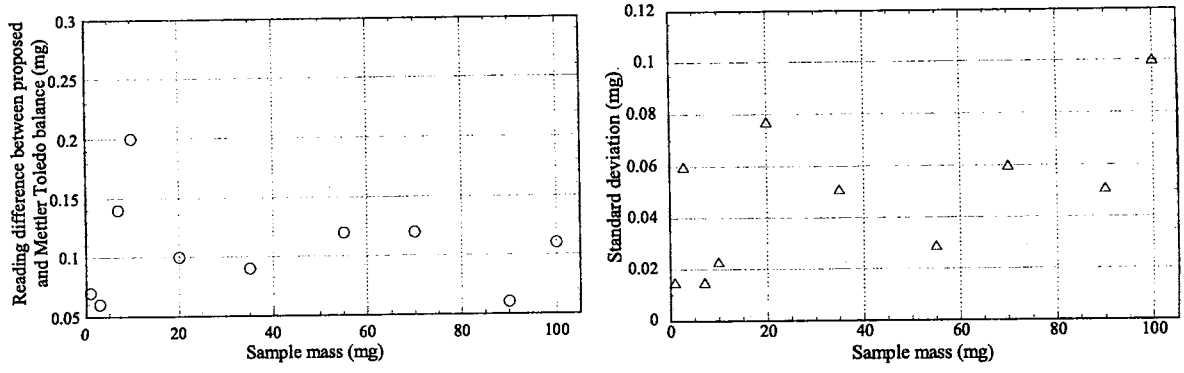

(a) Reading difference between the Proposed system and Mettler balance (b) Standard deviation of the proposed system

Fig. 17 Evaluation of the performances of the proposed system (accuracy and precision)

8.3 Development of an integration ant-windup technique of the beam control system

For the control systems which involve an integrator at the feed forward path, the problem of integration windup arises where an input constraint is included to protect the system. The integration windup affects the system performances and decreases the ability of the system to reject the external disturbances which sometimes leads to insatiability. An anti windup scheme is added to the beam control system as shown in Fig. 18 (a).

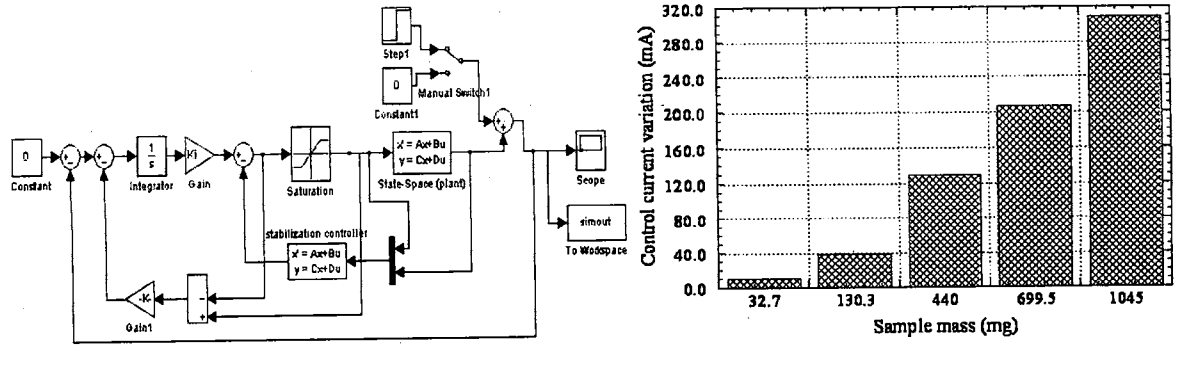

(a) Control system block diagram (b) Current vs. mass characteristics

Fig 18 Anti-windup scheme for the beam control system and system characteristics

After adding the anti-windup scheme, the system could reject large disturbances and this helps to increase the measurement capacity of the balance system. The experiments are carried out on the system and it is found that system capacity can reach 1g as shown in Fig. 18 (b).

9. Conclusion

The repulsive type magnetic bearing is right suited for manufacturing such system because of its non-contact operation which makes the system more sensitive than the conventional bearing balances. Moreover, it is single axis controlled and as result, a simplified control scheme is needed for completely stable levitation. The design principle depends on using a balance beam with two ends for the measuring, where at one end, the mass holder is located and an actuator is located on the other. This enables the user to eliminate the effect of gravity and as a result, measures the mass of the sample. The balance beam is designed so that the sample holder and the actuator are distant; so this system can be used to detect the change in the mass of a sample as a function of a controlled temperature and/ or time which is known as thermogravimeteric analysis (TGA). The experimental results confirmed that the system can measure the mass of the samples with satisfactory measurement performances.

In future, the plan of work will concern with using another control design technique such as H-∞ control which considers the model uncertainty such as unmodeled high frequency dynamics, neglected non-linearties, and plant parameter perturbations due to environmental factors. Using such control technique will increase the system robustness and improve the system performances and as a result the measurement error decreases.

References

[1] A. Hussien, T. Okada, T. Ohji, S. Yamada, and M. Iawhara, "A repulsive-type magnetic bearing micro-mass measurement system and measurement of resolution", *Transaction of the Magnetic Society of Japan*, vol. 4, no. 2, pp. 51-55, 2004.

[2] Alaa A. Hussien, Tomotada Okada, Takahisa Ohji, Sotoshi Yamada and Masayoshi Iwahara, "Investigation of the configuration and control of a repulsive-type magnetic levitation system used for micro-mass measurement" *Proceeding of the 16th SEAD.*, June 2004, Kyushu, Japan.

[3] T. Okada, Alaa A. Hussien, T. Ohji, S.Yamada, and masayoshi Iwahara "A Permanent Magnet Repulsive Type Magnetic bearing Balance System" Proceedings *of the 3rd Japan Australia, New Zealand Joint Seminar on Applications of Electromagnetic Phenomena in Electrical and Mechanical systems.* pp. 53-57, January 2004, Auckland, New Zealand.

[4] A. Hussien, T. Okada, T. Ohji, M. Iawhara, and S. Yamada "Improvement of the measurement characteristics of a magnetic bearing balance system", *Transaction of the Magnetic Society of Japan*, vol. 5, no. 2, pp. 97-100, 2005.

[5] Alaa A. Hussien, S. Yamada, and M. Iawhara, T. Okada, and T. Ohji "Application of the repulsive-type magnetic bearing for manufacturing micromass measurement balance equipment", *IEEE Transaction of Magnetics*, vol 41, no. 10, pp. 3802-3804. Oct. 2005.

学位論文審査結果の要旨

当該学位論文に対して，平成18年7月31日に第1回論文審査委員会を開催し，同年8月1日に行われた口頭発表後に第2回論文審査委員会を開催し討議した結果，以下の通り判定した。

本研究は，1軸不安定特性をもつ永久磁石反発磁気軸受をデジタル制御により安定させた非接触磁気軸受と完全無摩擦の特徴を用いた精密微小質量測定への応用に関する研究である。小形化の可能な本磁気軸受機構による精密微小質量測定器の研究開発は，磁気軸受の特徴を最も発揮できるものとして工学的に重要であり，以下にその研究成果を列記する。

(1) 永久磁石反発磁気軸受の磁気回路構成の設計

永久磁石反発磁気軸受の磁気回路と反発力特性の関係について，磁気シャント回路を提案し3次元電磁界解析により特性の解析を行い，反発力，剛性，線形性などを制御した構成を設計した。

(2) 質量測定用のバランサビーム系の検討

測定質量用のバランサビーム系にボイスコイルモータを適用し，バランサビームの非接触での安定化，ならびに測定質量変化によるバランサ位置移動から生ずる誤差発生を抑制することを実現した。

(3) システムモデリングとデジタル制御

バランサの磁気軸受の制御ならびに質量測定のバランサビームの水平制御に対して，磁気系ならびに機械系のモデリングを行いデジタル信号処理による制御システムを実現した。

(4) 磁気軸受付質量測定器の性能の測定

同システムを実験によりその性能を評価した結果，計量質量1.0 g（最大）に対して，計量誤差10 μg，最小計量値30 μgの値を得た。

以上の研究は，提案する永久磁石反発磁気軸受の特徴を生かした高精密質量測定器を検討した内容であり，博士（工学）論文に値するものと判定した。